

## Intrinsically tunable 0.67BiFeO<sub>3</sub>-0.33BaTiO<sub>3</sub> thin film bulk acoustic wave resonators

A. Vorobiev,<sup>1,a)</sup> S. Gevorgian,<sup>1</sup> N. Martirosyan,<sup>2</sup> M. Löffler,<sup>3</sup> and E. Olsson<sup>3</sup>

<sup>1</sup>Department of Microtechnology and Nanoscience, Chalmers University of Technology, SE-41296 Gothenburg, Sweden

<sup>2</sup>Department of Microelectronics and Biomedical Devices, State Engineering University of Armenia, Teryan 105, 0009 Yerevan, Armenia

<sup>3</sup>Department of Applied Physics, Chalmers University of Technology, SE-41296 Gothenburg, Sweden

(Received 20 September 2012; accepted 14 November 2012; published online 4 December 2012)

Intrinsically tunable 0.67BiFeO<sub>3</sub>-0.33BaTiO<sub>3</sub> (BF-BT) thin film bulk acoustic wave resonators with record high tunability of 4.4% and effective electromechanical coupling coefficient of 10% are fabricated and analyzed. The analysis, based on the theory of the dc field induced piezoelectric effect with the mechanical loading by the electrodes taken into account, reveals that the enhanced parameters are associated with the inherently high BF-BT electrostriction coefficient, which is found to be  $5.9 \times 10^{10}$  m/F. The  $Q$ -factor of the BF-BT resonators is up to 220 at 4.1 GHz and is limited mainly by acoustic wave scattering at reflection from a relatively rough top interface.

© 2012 American Institute of Physics. [<http://dx.doi.org/10.1063/1.4769346>]

The electrically tunable thin film bulk acoustic wave resonators, utilizing electric field induced piezoelectric effect in paraelectric phase ferroelectrics Ba<sub>x</sub>Sr<sub>1-x</sub>TiO<sub>3</sub> (BSTO), have been intensively developed for the last five years.<sup>1-7</sup> The BSTO bulk acoustic wave solidly mounted resonators (BAW-SMRs), with an improved  $Q$ -factor reveal a product of the  $Q$  and frequency  $Qf \approx 1900$  GHz, which is already sufficient for practical applications in, e.g., tunable filters.<sup>8</sup> However, the tunability of the resonance frequency and effective electromechanical coupling coefficient of these BAW-SMRs, 2% and 4.4%, respectively, are still lower than required.<sup>7</sup> For applications in agile front ends of the advanced transceivers that are used in microwave communication systems, the tunability of the BAW resonators should be more than 5%. The required coupling coefficient is defined by the system bandwidth and it should be 6.5% and higher, for example, personal communication systems.<sup>9</sup> Recently, the BSTO BAW-SMRs with a tunability and coupling coefficient of 3.8% and 7.1%, respectively, have been reported, though their  $Qf \approx 720$  GHz is rather low.<sup>6</sup> The BAW resonators utilizing polar phase ferroelectric PZT revealed the highest tunability of 5% and a coupling coefficient of 30%.<sup>10,11</sup> However, the hysteresis, which is typically comparable with the tunability, significantly limits their applications. In this paper, we demonstrate that applying the recently developed model of the dc field induced piezoelectric effect (Ref. 1) to available material parameters allows a selection of the 0.67BiFeO<sub>3</sub>-0.33BaTiO<sub>3</sub> (BF-BT) multiferroic as the piezoelectric layer for BAW resonators with higher tunability and coupling coefficient.

In this model of the field induced piezoelectric effect in a non-loaded ferroelectric film, the following relation between the electromechanical coupling factor  $k_f^2$  and the relative tunability of permittivity  $n_r$  has been established<sup>1</sup>

$$k_f^2 \approx \frac{4q^2}{3c^0\beta} n_r, \quad (1)$$

where  $q$ ,  $\beta$ , and  $c^0$  are the corresponding components of the tensors of linear electrostriction, dielectric nonlinearity, and elastic constant at dc field  $E_{dc} = 0$ , respectively. The dc bias dependent tunabilities of the series ( $n_{sf}$ ) and parallel ( $n_{pf}$ ) resonance frequencies may be described in terms of  $n_r$  as<sup>1</sup>

$$n_{sf} = k_f^2 \left( \gamma + \frac{\mu}{2} + \frac{4}{\pi^2} \right), \quad (2)$$

$$n_{pf} = k_f^2 \left( \gamma + \frac{\mu}{2} \right), \quad (3)$$

where  $\gamma \approx m/8q^2\epsilon$ ,  $\mu \approx \epsilon^b/\epsilon$ ,  $m$  and  $\epsilon^b$  are the corresponding components of the tensors of nonlinear electrostriction and the background permittivity, respectively. It can be seen that the coupling factor and tunability of the resonance frequency are proportional to  $q^2$ . Thus, one way to increase the tunability and coupling factor is the selection of materials with a higher electrostriction coefficient. Simple calculations, using data of the direct piezoelectric effect measurements, indicate that the Mn modified BF-BT ceramic, for example, reveals  $q_{BF-BT} = 13.93 \times 10^{10}$  m/F, which is more than 10 times higher than the  $q_{BSTO} = 1.08 \times 10^{10}$  m/F of the Ba<sub>0.3</sub>Sr<sub>0.7</sub>TiO<sub>3</sub> ceramic.<sup>12,13</sup>

In this work, the BF-BT BAW-SMR test structures are fabricated on high resistive Si substrates with SiO<sub>2</sub>/W Bragg reflectors.<sup>8</sup> The BF-BT films are grown by pulsed laser deposition using a 0.1 wt. % MnO<sub>2</sub> doped 0.67BiFeO<sub>3</sub>-0.33BaTiO<sub>3</sub> target. The 100 nm thick Al and Pt layers are used as top and bottom electrodes, respectively. The top electrode diameter is 60  $\mu$ m. The thickness of the BF-BT films used in analysis below is 330 nm, unless otherwise indicated. The series ( $f_s$ ) and parallel ( $f_p$ ) resonance frequencies are determined at the maximum of the real parts of the complex admittance and impedance, respectively. The relative tunability of permittivity is

<sup>a)</sup>Author to whom correspondence should be addressed. Electronic mail: andrei.vorobiev@chalmers.se.

calculated as  $n_r = (\varepsilon(0) - \varepsilon)/\varepsilon(0)$ , where  $\varepsilon(0)$  is the permittivity at  $E_{dc} = 0$ . The tunability of the resonance frequency is calculated as  $n_{s(p)} = (f_{s(p)}(0) - f_{s(p)})/f_{s(p)}(0)$ , where  $f_{s(p)}(0)$  is the resonance frequency at electric field extrapolated to  $E_{dc} = 0$ . The effective electromechanical coupling coefficient of a loaded BAW-SMR is calculated as

$$k_{\text{eff}}^2 = \frac{\pi^2 f_p^2 - f_s^2}{8 f_p^2}. \quad (4)$$

According to Eqs. (1)–(3), the non-loaded tunability and coupling factor are linear functions of the relative tunability of permittivity. Fig. 1 shows the dependences of the permittivity of the BF–BT films on dc bias for one cycle of the dc bias voltage, measured at 1 MHz and at the resonance frequency of 4.2 GHz. The inset shows the frequency dependence of permittivity at  $E_{dc} = 0$ . It can be seen that there is rather strong frequency dispersion of permittivity with visible hysteresis at 1 MHz. The hysteresis at 4.2 GHz is significantly lower. The relative tunability of permittivity is reduced correspondingly from 39% down to 21%. This behaviour can be attributed to the contribution of irreversible polarization associated with domain wall vibrations with distributed relaxation frequency since the ceramic counterpart Curie temperature is 605 °C.<sup>14,15</sup> The weak resonance peak visible in the frequency dependence of permittivity without dc electric field (see inset in Fig. 1) is associated with a dc field independent part of the piezoelectric coefficient. This contribution is negligible in comparison with that of the dc field induced piezoelectric effect utilized in the considered intrinsically tunable BAW-SMRs.

Fig. 2 shows the tuning performance of the BF–BT BAW-SMRs. It can be seen that the series resonance frequency shifts down with the increasing dc bias field, which is in agreement with the theory.<sup>16</sup> The tunability of series resonance frequency is 4.4% and the effective electromechanical coupling coefficient is 10% at 14 V. Hysteresis of the series

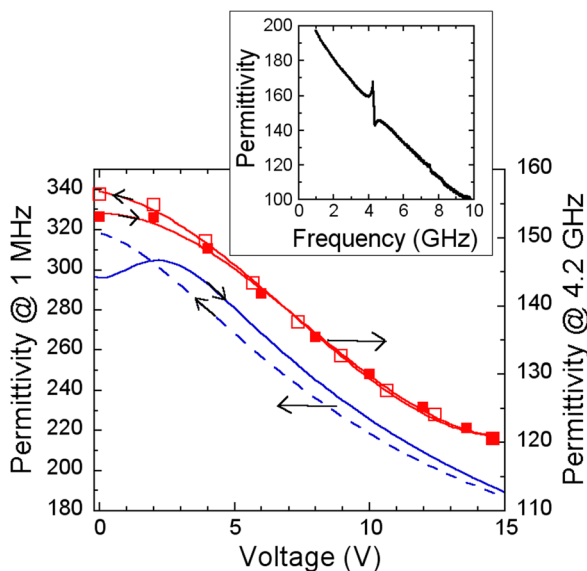


FIG. 1. Permittivity of the BF–BT films at 1 MHz and at a resonance frequency of 4.2 GHz vs. one cycle of dc bias voltage sweep varying according to arrow directions. Inset shows the frequency dependence of permittivity at  $E_{dc} = 0$ .

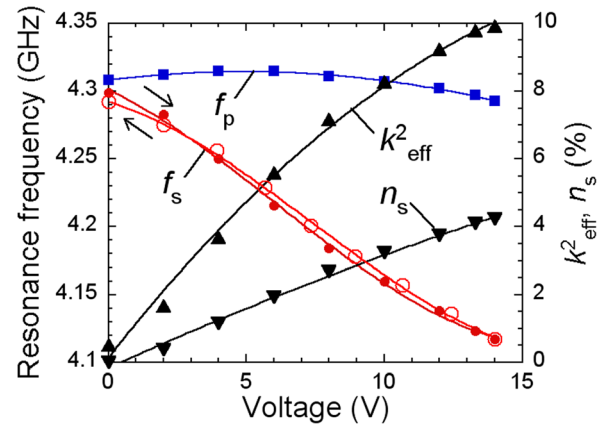


FIG. 2. Series ( $f_s$ ) and parallel ( $f_p$ ) resonance frequencies, tunability of the series resonance frequency  $n_s$ , and the effective electromechanical coupling coefficient  $k_{\text{eff}}^2$  of the BF–BT BAW-SMR vs. dc bias voltage. One cycle of the series resonance frequency dependence, varying according to arrow directions, is shown.

resonance frequency is below 0.2%, which is much less than the tunability and can be ignored for practical applications. These  $n_s$  and  $k_{\text{eff}}^2$  values are the highest that have been reported so far for intrinsically tunable BAW resonators without hysteresis. The parallel resonance frequency reveals much weaker field dependence with a tunability of only 0.35%. This is in agreement with Eqs. (2) and (3), assuming that  $\gamma + \mu/2 \ll 1$ , which makes  $4/\pi^2$  the leading term in Eq. (2).<sup>16</sup>

The mechanical load of the piezoelectric layer, by the electrodes, results in reduced values of the BAW resonator tunability and effective electromechanical coupling coefficient in comparison with the intrinsic parameters due to the loss of acoustic energy in the non-piezoelectric electrodes.<sup>16,17</sup> However, modelling has shown that the dc bias field dependence of the resonance behaviour of the loaded piezoelectric layer follows the same trend as in the non-loaded case.<sup>16</sup> Thus, the BAW resonator tunability of resonance frequency and effective electromechanical coupling coefficient remain linear functions of the relative tunability of permittivity as in Eqs. (1)–(3). Fig. 3 shows the effective electromechanical coupling coefficient of the BF–BT BAW-SMR versus relative tunability of the permittivity. For comparison, the corresponding data for a BAW-SMR based on a 290 nm thick  $\text{Ba}_{0.25}\text{Sr}_{0.75}\text{TiO}_3$  film deposited by magnetron sputtering are also shown.<sup>7</sup> It can be seen that both dependences can be approximated by linear functions. The slope is larger for the BF–BT BAW-SMR, which implies a 10 times larger coupling coefficient at the same relative tunability. The main reason for this is higher proportionality coefficient in Eq. (1). Our calculations show that the parameters  $\beta$  and  $c^0$  of both materials do not differ much and, hence, the 10 times larger coupling coefficient of the BF–BT BAW-SMR is associated mainly with the larger electrostriction coefficient  $q$ . It should be noted that the relative tunability of permittivity of the BF–BT films is limited in comparison with that of the BSTO films (Fig. 3) by the break down field, which is more than 3 times lower than that currently achieved in the BSTO BAW-SMRs  $E_{dc} = 170 \text{ V}/\mu\text{m}$ .<sup>7</sup>

Subtracting Eqs. (2) and (3) gives tunability difference

$$n_{\text{sf}} - n_{\text{pf}} \approx \frac{4}{\pi^2} k_{\text{f}}^2. \quad (5)$$

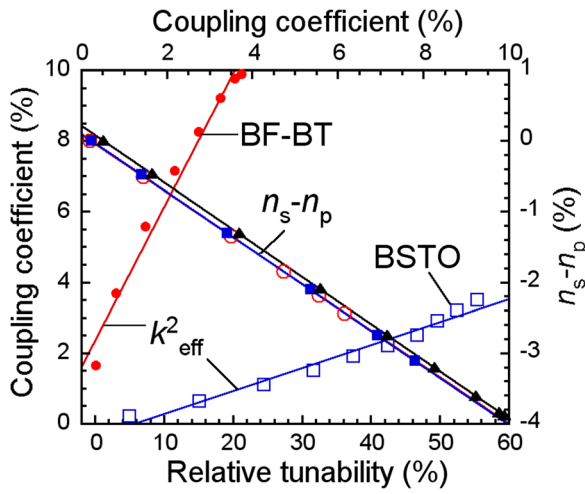


FIG. 3. Effective electromechanical coupling coefficient  $k_{\text{eff}}^2$  of the BF–BT BAW-SMR vs. relative tunability of permittivity (solid circles) and tunability difference  $n_s - n_p$  vs. effective electromechanical coupling coefficient of the BF–BT BAW-SMRs with different BF–BT film thicknesses: 198 nm (open circles), 264 nm (solid squares), and 330 nm (triangles). The  $k_{\text{eff}}^2$  of the BSTO BAW-SMR vs. relative tunability of permittivity (open squares) is also shown.

Fig. 3 shows the BAW-SMR tunability difference versus effective electromechanical coupling coefficient of the BF–BT BAW-SMRs with different BF–BT film thicknesses: 198 nm, 264 nm, and 330 nm. It can be seen that the dependences are linear with the same slope of approximately 0.41, which is very close to the  $4/\pi^2 = 0.405$  predicted by theory for the non-loaded piezoelectric layer, see Eq. (5).<sup>1</sup> This confirms the validity of the model in the case of the BF–BT films. Additionally, one can conclude that the BAW-SMR tunability difference and coupling coefficient are the same functions of the electrode thickness in the whole thickness range starting from zero.

Fig. 4 shows the effective electromechanical coupling coefficient versus the relative tunability of permittivity for different thicknesses of the BF–BT film. It can be seen that for smaller thicknesses of the BF–BT film, the coupling coefficient is smaller. This trend demonstrates the effect of loading of the BAW resonators by electrodes since a change in

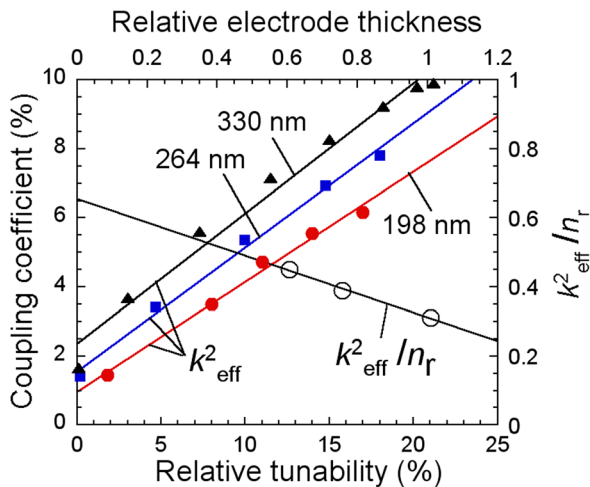


FIG. 4. Effective electromechanical coupling coefficient  $k_{\text{eff}}^2$  vs. relative tunability of permittivity  $n_r$  for different BF–BT film thicknesses and ratio of  $k_{\text{eff}}^2$  and  $n_r$  vs. relative electrode thickness.

the thickness of the BF–BT film can be interpreted as a relative change in the electrode thicknesses. As mentioned above, this effect results in a reduction in the acoustic energy in the piezoelectric film relative to the energy in the passive electrodes.

Analysis of Eq. (1) indicates that the electrostriction coefficient  $q$  can be evaluated, for example, by extrapolating the electrode thickness dependence of the effective electro-mechanical coupling coefficient to zero electrode thickness. Fig. 4 shows the dependence of the ratio  $k_{\text{eff}}^2/n_r$  on the relative thickness of the electrodes  $(t_{\text{Al}} + t_{\text{Pt}})/t_{\text{BF-BT}}$ . As seen, a linear extrapolation of this dependence gives  $k_{\text{eff}}^2/n_r = 0.65$  at zero electrode thickness. Using Eq. (1), one obtains  $q = 5.9 \times 10^{10}$  m/F which is 5 times larger than the  $q_{\text{BSTO}}$ .<sup>13</sup> Similar extrapolations made for tunability and coupling coefficient give the corresponding parameters of the non-loaded BF–BT film:  $n_{\text{sf}} = 5.4\%$ ,  $k_{\text{eff}}^2 = 14\%$ . The tunability and coupling coefficient of the BF–BT BAW-SMRs can be further improved in, at least, two ways or their combination. The first is to increase the breakdown field up to the values currently achieved in the BSTO BAW-SMRs, where  $E_{\text{dc}} = 170$  V/ $\mu\text{m}$  (Fig. 3), by proper doping and/or interface optimization. This will allow for the application of a higher dc bias and increase the tunability up to  $n_s = 15\%$  and the coupling coefficient up to  $k_{\text{eff}}^2 = 30\%$ , in the case of using the conventional electrode design. A second possibility is to use composite electrodes with lower acoustic thickness, such as, e.g., W/Pt, which concentrates the acoustic wave in the piezoelectric layer and, thereby, increases the tunability and coupling coefficient up to non-loaded values.<sup>17</sup>

The  $Q$ -factors of the BF–BT BAW-SMRs at series ( $Q_s$ ) and parallel ( $Q_p$ ) resonances have been evaluated as

$$Q_{s,p} = \frac{1}{2} f_{s,p} \left. \frac{\partial \varphi}{\partial f} \right|_{f=f_{s,p}}, \quad (6)$$

where  $\varphi$  is the phase of impedance. The measured  $\varphi$  is shown in Fig. 5 in the frequency range of resonances at different dc bias voltages. The corresponding  $Q_s$  and  $Q_p$  calculated using Eq. (6) are shown in Fig. 6.

The  $Q$ -factors approach zero values at low dc fields due to the nature of the field induced piezoelectric effect. To determine the  $Q$ -factor associated with acoustic loss only

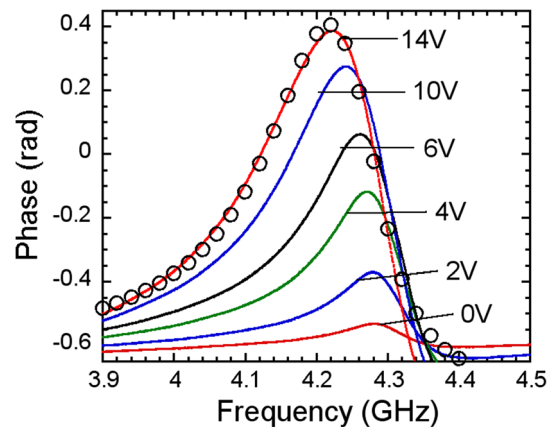


FIG. 5. The phase of impedance at different dc bias voltages. Shown also is the best fit to the mBVD model (open circles) at 14 V dc bias.

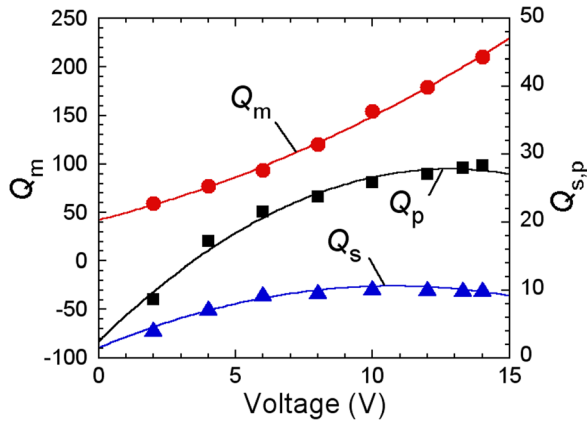


FIG. 6. The quality factors at series  $Q_s$  and parallel resonances  $Q_p$  vs. dc bias voltage. Shown also is the calculated mechanical quality factor  $Q_m$ .

( $Q_m$ ), we analyzed the modified Butterworth-Van Dyke (mBVD) circuit model shown in Fig. 7.

The indexes “m” and “0” denote the motional and dielectric arms, respectively. The parameters of the mBVD equivalent circuit have been found by fitting the calculated phase of impedance to the measured values. The best fits have been obtained by taking into account the extrinsic series resistance ( $R_s$ ), parasitic inductance ( $L_s$ ), and parallel capacitance ( $C_p$ ) associated with the measurement setup, as shown in Fig. 7. As an example, the phase of impedance calculated for 14 V dc bias is shown in Fig. 5 by open circles. The corresponding mBVD circuit parameters are given in Table I. The definition (6) allows expression of the  $Q$ -factors in terms of the mBVD circuit parameters, ignoring the parasitic  $C_p$  and  $L_s$ , as<sup>18</sup>

$$Q_s = \frac{\omega_s L_m}{R_s + R_m}, \quad (7)$$

$$Q_p = \frac{\omega_p L_m}{R_0 + R_m}, \quad (8)$$

and calculation of the purely mechanical  $Q$ -factor as

$$Q_m = \frac{\omega_s L_m}{R_m}. \quad (9)$$

Fig. 6 shows  $Q_m$  calculated using Eq. (9). The  $Q_s$  and  $Q_p$  are significantly lower than the  $Q_m$  values since  $R_s$  and  $R_0$  dominate over  $R_m$ , see Eqs. (7), (8), and Table I. The  $R_0$  represents dielectric losses in the BF–BT film. For comparison, the loss tangent of the BF–BT bulk counterpart calculated using the virtual crystal approximation corresponds to  $R_{0\text{-bulk}} \approx 0.7$ , at 4 GHz.<sup>19,20</sup> The  $R_0 \approx 0.9$  is fairly comparable with

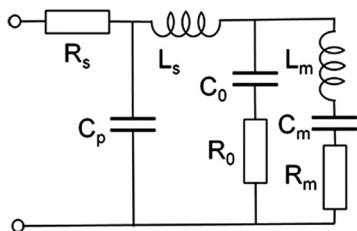


FIG. 7. The mBVD equivalent circuit of a BF–BT BAW–SMR test structure.

TABLE I. The mBVD circuit parameters of a BAW–SMR test structure at 14 V dc bias.

$R_s$	$C_0$	$R_0$	$L_m$	$C_m$	$R_m$	$L_s$	$C_p$
5.5 $\Omega$	9.15 pF	0.9 $\Omega$	1.55 nH	0.99 pF	0.19 $\Omega$	–50 pH	0.7 pF

that of the bulk and slightly higher due to extrinsic losses associated with structural imperfections typical for thin films. The series resistance  $R_s = 5.5 \Omega$  in our BAW–SMR test structures is mainly composed of the contact resistance between the probe tips and the Al top electrodes  $R_c \approx 4.8 \Omega$ . This indicates that the  $R_s$  is rather an artifact of the measurements but not an intrinsic BAW–SMR parameter. In a more complex BAW–SMR design, with Au leading electrodes, the  $R_s$  can be reduced below  $R_m$  and, correspondingly, the  $Q_s$  can approach the  $Q_m$  values. It can be seen that the  $Q_m \approx 220$  at 14 V, which results in the product  $Qf \approx 920$  GHz. It is among the highest reported so far for the intrinsically tunable BAW resonators. It is much higher than that of varactor based tunable  $LC$  resonators. Our resonators already may be used in voltage controlled oscillators and some tunable filters instead of  $LC$  tanks.<sup>21</sup> However, the  $Q$ -values are still lower than those required for applications in microwave transceiver front ends.

Fig. 6 reveals a rather linear dc bias field dependent  $Q_m$ , indicating that it can be significantly improved by increasing the BF–BT film breakdown field. On the other hand, modeling of the surface roughness induced attenuation of reflected acoustic waves using the measured BF–BT film surface roughness  $\eta_{rms} = 12.5$  nm gives  $Q_{sc} = 340$ .<sup>22</sup> This means that our BF–BT BAW–SMR  $Q$ -factor is mainly defined by acoustic losses associated with wave scattering upon reflection from the relatively rough top interface. Our preliminary analysis indicates that the BF–BT film surface roughness is mainly defined by the faceting tips of (111) oriented columnar grains. The amount of these grains can be controlled by changing the substrate position with respect to the plume axis during deposition. Thus, future plans include the improvement of the quality of the BF–BT films and interfaces in terms of the breakdown field, roughness, and optimization of the electrode design.

This work was partially supported by the Swedish Research Council Projects 2009-3460 and 2011-4203.

<sup>1</sup>A. Noeth, T. Yamada, P. Murali, A. K. Tagantsev, and N. Setter, *IEEE Trans. Ultrason. Ferroelectr. Freq. Control* **57**, 379 (2010).

<sup>2</sup>S. A. Sis, V. Lee, J. D. Phillips, and A. Mortazawi, *IEEE MTT-S Int. Microwave Symp. Dig.* **2012**, 1.

<sup>3</sup>G. N. Saddik, J. Son, S. Stemmer, and R. A. York, *J. Appl. Phys.* **109**, 091606 (2011).

<sup>4</sup>A. Volatier, E. Defay, M. Aid, A. N’hari, P. Ancey, and B. Dubus, *Appl. Phys. Lett.* **92**, 032906 (2008).

<sup>5</sup>B. Ivira, A. Reinhardt, E. Defay, and M. Aid, in *IEEE International Frequency Control Symposium* (2008), p. 254.

<sup>6</sup>J. Berge and S. Gevorgian, *IEEE Trans. Ultrason. Ferroelectr. Freq. Control* **58**, 2768 (2011).

<sup>7</sup>A. Vorobiev, S. Gevorgian, M. Löffler, and E. Olsson, *J. Appl. Phys.* **110**, 054102 (2011).

<sup>8</sup>A. Vorobiev and S. Gevorgian, *Appl. Phys. Lett.* **96**, 212904 (2010).

<sup>9</sup>R. Aigner and L. Elbrecht, *RF Bulk Acoustic Wave Filters for Communications*, edited by K.-Y. Hashimoto (Artech House, Norwood, MA, 2009), p. 91.

- <sup>10</sup>J. Conde and P. Muralt, *IEEE Trans. Ultrason. Ferroelectr. Freq. Control* **55**, 1373 (2008).
- <sup>11</sup>M. Schreiter, R. Gabl, D. Pitzer, R. Primig, and W. Wersing, *J. Eur. Ceram. Soc.* **24**, 1589 (2004).
- <sup>12</sup>S. O. Leontsev and R. E. Eitel, *J. Am. Ceram. Soc.* **92**, 2957 (2009).
- <sup>13</sup>A. Noeth T. Yamada, A. K. Tagantsev, and N. Setter, *J. Appl. Phys.* **104**, 094102 (2008).
- <sup>14</sup>A. Vorobiev, T. Ahmed, and S. Gevorgian, *Integr. Ferroelectr.* **134**, 111 (2012).
- <sup>15</sup>S. O. Leontsev and R. E. Eitel, *J. Mater. Res.* **26**, 9 (2011).
- <sup>16</sup>A. Noeth, T. Yamada, V. O. Sherman, P. Muralt, A. K. Tagantsev, and N. Setter, *J. Appl. Phys.* **102**, 114110 (2007).
- <sup>17</sup>S. Gevorgian and A. Vorobiev, in *Proceedings of the 40th European Microwave Conference, EuMC 2010; 13th European Microwave Week 2010, EuMW2010: Connecting the World, Paris, 28 September–30 September* (2010), pp. 1210–1213.
- <sup>18</sup>J. Kaitila, *RF Bulk Acoustic Wave Filters for Communications*, edited by K.-Y. Hashimoto (Artech House, Norwood, MA, 2009), p. 58.
- <sup>19</sup>Yu. E. Roginskaya, Yu. Ya. Tomashpol'skii, Yu. N. Venetsev, V. M. Petrov, and G. S. Zhdanov, *Sov. Phys. JETP* **23**, 47 (1966) (in English).
- <sup>20</sup>O. G. Vendik, E. K. Hollmann, A. B. Kozyrev, and A. M. Prudan, *J. Supercond.* **12**(2), 325 (1999).
- <sup>21</sup>M. A. Copeland, S. P. Voinigescu, D. Marchesan, P. Popescu, and M. C. Maliepaard, *IEEE Trans. Microwave Theory Tech.* **48**, 170 (2000).
- <sup>22</sup>P. B. Nagy and L. Adler, *J. Acoust. Soc. Am.* **82**, 193 (1987).